



Pressure Vessels Structural Integrity Assessment Using Failure Analysis Diagrams

Rocha Pinto^{a*}, J. J.; Mattar Neto^{b**}, M.

^a Navy Technological Center in São Paulo - 18560-000, Iperó, SP, Brazil.

^b Institute of Energy and Nuclear Research - 05508-900, São Paulo, SP, Brazil

Correspondence: *juarezpinto14@gmail.com **mmattar@usp.br

Abstract: There is much discussion today about the possibility of extending the lifetime of industrial plant components due to economic factors. Pressure vessels are among the most expensive components, and their replacement can significantly impact the operation of an entire plant. In this context, several Fitness-for-Service (FFS) methodologies can be applied to assess structural integrity, addressing not only economic aspects but also enhancing safety. Failure Assessment Diagrams (FADs) are widely used in FFS methodologies to prevent future failures by analyzing crack-type defects. These diagrams establish acceptability criteria based on the material toughness ratio and loading ratio. Recommended practices utilizing the BS-7910, API-579, and R6 methodologies are addressed in this work, alongside principles from fracture mechanics, material properties, and solid mechanics. The main objective was to develop computer programs in Matlab to analyze a case study involving a pressure vessel manufactured from SA-516 Gr 70 steel, determining the critical dimensions of semi-elliptical cracks in longitudinal and circumferential orientations of a cylindrical section. Level 2 evaluation, the most commonly used in FFS methodologies, was applied to develop the programs. This study enabled the creation of tools to automate calculations and generate FAD graphs, considering the critical depth and length of cracks. These tools support decision-making in structural design requirements and provide a means of evaluating equipment in service with crack-type defects, extending its operational lifetime. The FFS methodologies studied are based on ASME Codes for pressure vessels and piping, particularly Sections III and XI. Based on the analysis of API-579, BS-7910, and R6 methodologies under the operating conditions of the case study, it is possible to conclude that, for normal evaluations, critical length ($2c$) = 40.64 mm and critical depth (a) = 10.16 mm are acceptable values. However, for evaluations requiring safety considerations under the R6 procedure, applicable to Class A service equipment in the nuclear sector, only critical length (l) = 5 mm and depth (a) = 2.5 mm are permissible values.

Keywords: failure assessment diagram, fitness-for-service, BS-7910, API-579, R6, crack, pressure vessel.



Avaliação da Integridade Estrutural de Vasos de Pressão com a Utilização dos Diagramas de Análise de Falhas

Resumo: Muito se discute atualmente, acerca da possibilidade da extensão da vida útil de componentes de plantas industriais motivado por fatores econômicos. Os vasos de pressão são os componentes de maior custo e a sua substituição pode impactar o funcionamento de toda a planta. Nesse contexto várias metodologias de adequação ao serviço “Fitness For Service” (FFS) podem ser utilizadas para a avaliação da integridade estrutural, não somente visando a aspectos econômicos, mas também aumento da segurança. Os diagramas de análise de falhas “Failure Assessment Diagram” (FAD), são os mais empregados nas metodologias FFS para prevenção futura de uma falha a partir da consideração de um defeito do tipo trinca, estabelecendo um critério para aceitabilidade dos defeitos baseados na razão de tenacidade do material e razão de carregamento. As práticas recomendadas que utilizem as metodologias da BS-7910, API-579 e R6 foram abordadas neste trabalho, além de disciplinas no campo da mecânica da fratura, propriedades dos materiais, e mecânica dos sólidos, tendo como objetivo principal a elaboração de programas computacionais utilizando a linguagem Matlab, no estudo de caso de um vaso de pressão fabricado em aço SA-516 Gr 70 para determinar as dimensões críticas de trinca semi elíptica, dispostas nos sentido longitudinal e circunferencial da seção cilíndrica. O nível de avaliação dois que é o mais empregado nas metodologias FFS foi utilizado para elaboração dos programas computacionais. Este trabalho possibilitou o desenvolvimento de ferramentas para automatizar os cálculos e apresentação dos gráficos FAD, considerando a profundidade e comprimento crítico da trinca, favorecendo a tomada de decisão nos requisitos do projeto estrutural assim como proporcionar meios de avaliação de equipamento em serviço, com defeito do tipo trinca na extensão de sua vida útil. É possível observar também que as metodologias FFS estudadas são fundamentadas nos Códigos ASME para vasos de pressão e tubulações, principalmente nas Seções III e XI. Na análise das metodologias API-579, BS-7910 e R6 considerando as condições de operação do estudo de caso são possíveis concluir que para avaliações normais o valor de $(2c) = 40.64$ mm e $(a) = 10.16$ mm respectivamente para comprimento e profundidade críticos pode ser admitido, porém em um uma avaliação com requisitos de segurança do procedimento R6, referente a equipamento da classe de serviço A da área nuclear, somente pode ser aceito $(l) = 5$ mm e $(a) = 2.5$ mm respectivamente para comprimento e profundidade críticos.

Palavras-chave: failure assessment diagram, fitness-for-service, BS-7910, API-579, R6, trinca, vaso de pressão.

1. INTRODUCTION

Pressure vessels are of fundamental importance in the oil refining, gas, nuclear, chemical, thermoelectric, and sugar and alcohol industries. These equipment components are used to process flammable, toxic, explosive, and radioactive materials under high-pressure and high-temperature conditions. Accidents in such scenarios pose significant risks to the safety of operators, industrial plants, and the environment, with potential for catastrophic outcomes and substantial economic losses. Due to the severe consequences of pressure vessel failure, strict control of operating conditions is essential. Inspections using NDT (Non-Destructive Testing) methods are conducted to detect potential defects. Any defect identified during the equipment's service life must be evaluated to determine its acceptability or whether corrective actions, such as repair, operational adjustments, or decommissioning, are required [21]. The purpose of assessing structural integrity is to prevent future failures by evaluating structural damage using detailed inspection techniques and analysis procedures. These processes help extend the plant's safe operational period and the useful life of its components [6] [21].

The most widely used FFS methodologies for structural integrity assessment serve as guides for evaluating defect acceptability. According to [6], these include BS-7910 [1], API-579-1/ASME FFS-1 [2], and R6 [3] [4]. These methodologies are grounded in standards such as ASME Codes Sec. VIII Div. 1 and 2 [8] [9], Sec. III [5], BS PD 5500 [11], and mainly ASME Code Sec. XI [16]. ASME Sec. XI provides comprehensive procedures for evaluating equipment degradation during service and addressing deficiencies from original manufacturing, serving as a reference for all FFS methodologies. The disciplines of material properties, fracture mechanics, statistics, and finite element methods form the foundation of FFS methodologies. Plasticity restriction at the crack tip is a term used to represent the degree

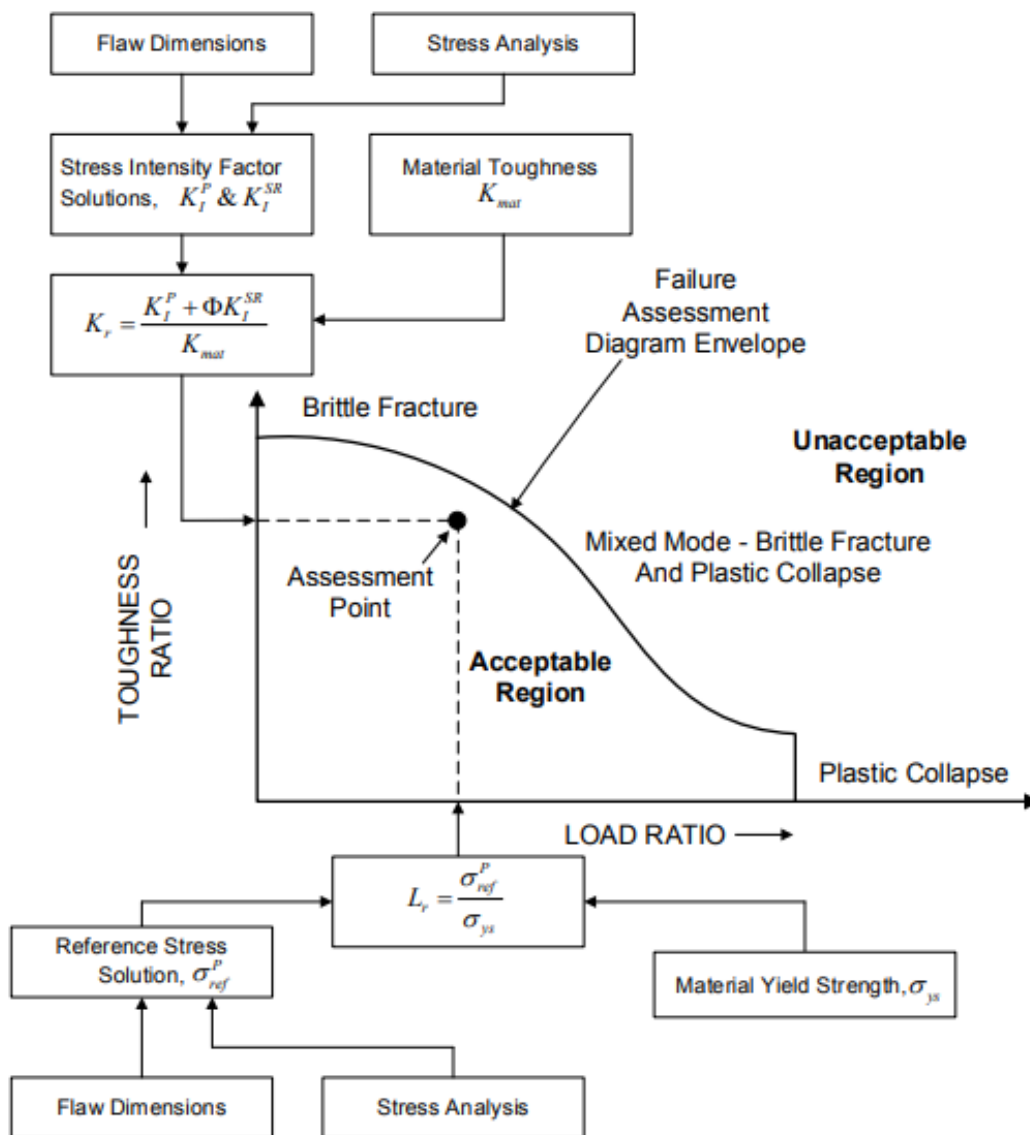
of triaxiality in the stress field; the greater the plasticity restriction, the higher the triaxiality [11] [19]. Procedures for calculating fracture toughness and assessing structural integrity typically assume conditions of high restriction at the crack tip, which tends to be conservative and may lead to overly cautious and uneconomical predictions. However, in cases where the geometry of the analyzed structure and the applied load result in significant loss of restriction, the material's toughness can increase in real-world applications [6].

FFS methodologies are employed to perform quantitative engineering assessments to demonstrate the structural integrity of an in-service component containing a crack or damage, ensuring it continues operating under specified conditions to avoid failure [2]. API-579 and BS-7910 are widely recognized standards in the oil and gas industry, providing comprehensive guidelines and primarily utilizing level 2 assessments [1] [2]. The R6 procedure, on the other hand, is most commonly used in the nuclear industry for inspecting critical equipment to ensure structural integrity [3] [4]. These FFS methodologies are frequently applied by engineering companies that offer consulting services in areas such as in-service monitoring, post-failure analysis, remaining life assessment, and equipment repair solutions [1] [2] [3] [4].

The objective of this work is to develop computer programs using Matlab software to automate calculations and determine the critical dimensions of semi-elliptical surface cracks in pressure vessels, in accordance with FFS methodologies, by employing Failure Analysis Diagrams (FAD). The defect is assumed to be located only in the cylindrical section of the pressure vessel, oriented parallel to the longitudinal weld bead and sufficiently far from structural discontinuities, nozzles, and inspection windows. The FAD approach is arguably the most widely used method for analyzing the elastoplastic fracture mechanics of structural components within FFS methodologies. This approach simplifies the highly nonlinear problem of elastoplastic fracture by using two parameters that vary with the applied load, covering a wide range of material behavior—from brittle fracture under linear elastic conditions to ductile overload in the fully plastic regime. The FAD method is particularly

suitable for welded components, as it accounts for residual stresses and can also be employed in ductile rupture analysis [11]. According to the ASME Code Sec. XI, the purpose of the FAD diagram is to evaluate cracks and discontinuities by establishing a criterion for defect acceptability. The ordinate of the diagram, K_r represents the toughness ratio, which is the ratio of the stress intensity factor K_I to the material toughness factor K_{mat} as described in Equation (1) [1] [2] [3] [4] [12] [16]. The FAD diagram is shown in Figure 1

Figure 1 - Failure analysis diagram



Source : Printscreen from API 579-1/ASME FFS-1:2016 [2].

The abscissa of the FAD diagram is represented by the factor L_r , which is defined as the ratio between the reference stress σ_{ref} and the material's yield stress σ_y , as described in Equation (2). In the ASME Code Sec. XI, this factor is referred to as S_r [1] [2] [3] [4] [12] [16].

$$K_r = \frac{K_I}{K_{mat}} \quad (1)$$

$$L_r = \frac{\sigma_{ref}}{\sigma_y} \quad (2)$$

Plastic collapse in a structure occurs in ductile materials when $L_r = 1$. Failure in brittle materials, on the other hand, occurs when $K_r = 1$. In mixed-mode scenarios, failure can occur with K_r and L_r less than 1, provided the evaluated point is located outside the acceptable region defined by a limiting curve determined by the material properties [1].

2. MATERIALS AND METHODS

The object of study is a pressure vessel, where the critical lengths and depths of semi-elliptical cracks will be determined under operating conditions using a flowchart relevant to Level 2 of the FFS methodology. Level 2 is widely applied and suitable for most cases.

The damage tolerance philosophy allows cracks to remain in the structure as long as they are significantly below critical size. Once the critical crack size is estimated, a safety factor is applied to determine the tolerable size [7]. The safety factor accounts for uncertainties in input parameters caused by primary damage mechanisms, which generally include embrittlement, corrosion, fatigue, and creep [22].

According to ASME Code Sec. III [5], stresses acting on pressure vessel walls are categorized into primary, secondary, and peak stresses, each with subcategories:

- Primary stresses are normal or shear stresses required to satisfy the laws of static equilibrium between internal and external forces and moments. These stresses are

induced by mechanical loads, such as weight, internal pressure, and wind. Catastrophic failures are often associated with primary stresses, as they are not self-limiting. Primary stresses are subdivided into:

Membrane stress P_m : Normal stresses that remain constant throughout the vessel wall thickness.

Bending stress P_b : Normal stresses arising from wall bending [17].

- Secondary stresses Q are normal or shear stresses caused by mechanical loads or thermal expansion due to geometric constraints in the pressure vessel. Secondary stresses are self-limiting and self-equilibrating, ensuring structural continuity. These stresses typically occur at discontinuities, residual welding areas, or as thermal stresses, and are further divided into:

Membrane stresses Q_m

Bending stresses Q_b

- Peak stresses F_P are localized stresses at points of stress concentration. These stresses can lead to crack initiation, stress corrosion cracking, or brittle fractures [17].

Damage mechanisms play a critical role in assessing structural integrity. Common mechanisms that initiate and propagate cracks in pressure vessels and pipelines include welding defects, brittle fractures, creep, thermal fatigue, thermal shock, erosion, corrosion, cavitation, mechanical fatigue, stress corrosion cracking, hydrogen-induced embrittlement, and radiation-induced embrittlement [1] [2]. Fracture mechanics provides tools for determining stress intensity factors K_I and material toughness K_{mat} . The calculation of K_I for external semi-elliptical cracks is prescribed by the ASME Code Sec. XI for pressure vessels, as shown in Equation (3) [15] [16]. This calculation is applied with variables specific to each FFS methodology, as outlined in Equations (4), (5), and (6) [1] [2] [3] [4].

$$(ASME Sec. XI) K_I = \{\sigma_m M_m + \sigma_b M_b\} \sqrt{\frac{\pi a}{Q}} \quad \text{or} \quad K_I = [(A_0 + A_p)G_0 + A_1 G_1 + A_2 G_2 + A_3 G_3] \sqrt{\frac{\pi a}{Q}} \quad (3)$$

$$(BS 7910) \quad K_I = M f_w \{M_m P_m + M_b P_b\} \sqrt{\pi a} \quad (4)$$

$$(API 579) \quad K_I = \frac{P R_i^2}{R_o^2 - R_i^2} \left[2G_0 - 2G_1 \left(\frac{a}{R_o}\right) + 3G_2 \left(\frac{a}{R_o}\right)^2 - 4G_3 \left(\frac{a}{R_o}\right)^3 + 5G_4 \left(\frac{a}{R_o}\right)^4 \right] \sqrt{\frac{\pi a}{Q}} \quad (5)$$

$$(R6) \quad (K_I^P) = \sqrt{\pi a} (\sigma_o^p f_o^A) \quad \text{and} \quad (K_I^S) = \sqrt{\pi a} (\sigma_o^s f_o^A + \sigma_1^s f_1^A) \quad (6)$$

The calculation of the toughness ratio (K_r) in the ASME Code Sec. XI is defined in Equation (7), along with other terms outlined in Topic C-4312, which specifically addresses axial cracks. The factor K_r in the BS-7910, API-579, and R6 methodologies is calculated using Equations (8), (9), and (10), respectively, each considering terms specific to their methodology.

$$(ASME Sec. XI) \quad K_r' = \sqrt{\frac{1000 K_I^2}{\left(\frac{E}{1-\nu}\right)^2 J_{IC}}} \quad \text{considering} \quad K_I = \left(\frac{p R_m}{t}\right) \sqrt{\frac{\pi a}{1000 Q}} * F \quad (7)$$

$$(BS 7910) \quad K_r = \frac{K_I^P + V K_I^S}{K_{mat}} \quad (8)$$

$$(API 579) \quad K_r = \frac{K_I^P + \Phi K_I^S}{K_{mat}} \quad (9)$$

$$(R6) \quad K_r = \frac{(K_I^P) + (K_I^S)}{K_{mat}} + \rho \quad (10)$$

The calculation of the loading ratio (S_r) in ASME Code Sec. XI [16] for axial surface cracks incorporates the term SF_m , which corresponds to the safety factor, as defined in Equation (11). In the R6 procedure [3] [4], this term is designated as (L_r) and is defined in Equation (12). The variables used in the R6 methodology are derived from those in the ASME Code Sec. XI [16], including factors employed in safety evaluations. These are applied to the material curve $f(L_{r_{safe}})$, along with safety factors extracted from the ASME Code Sec. III [5].

$$(ASME Sec. XI) \quad S_r = \frac{SF_m * \sigma_h}{\sigma_f} = \frac{SF_m \left(\frac{p * R_m}{t} \right)}{\left(\frac{\sigma_y + \sigma_u}{2} \right)} \quad (11)$$

$$(R6) \quad L_r = \frac{(1 - \zeta)^{1,58} \frac{\sigma_b}{3} + \sqrt{(1 - \zeta)^{3,16} \frac{\sigma_b^2}{9} + (1 - \zeta)^{3,14} \sigma_m^2}}{(1 - \zeta)^2 \sigma_y} \quad (12)$$

$$\text{considering:} \quad \zeta = \frac{a * l}{t(l + 2t)}$$

The reference stress factor (σ_{ref}) applied in calculation of the loading ratio for axial surface cracks in BS-7910 and API-579 methodologies is given according to equations (13) and (14), considering variables of each methodology.

$$(BS 7910) \quad \sigma_{ref} = M_s P_m + \frac{2P_b}{3(1 - \alpha'')^2} \quad (13)$$

$$(API 579) \quad \sigma_{ref}^p = \frac{gP_b + [(gP_b)^2 + 9(M_s P_m (1 - \alpha)^2)^2]^{0,5}}{3(1 - \alpha)^2} \quad (14)$$

Horizontal vessels are supported by saddles welded to the shell. The design considers loads due to internal pressure, moments, and shear forces related to the weight of the vessel and the reactions at the supports. These are calculated using the method proposed by L. P. Zick [14], which has been adopted as the calculation method in the ASME and BS PD5500 standards.

The limit curve of the FAD diagram for pressure vessels in ASME Code Sec. XI [16] is defined by points with coordinates (S_r , K_r) as given in Table K-4320-1, with a cut-off limit of $S_r=1.35$ for axial cracks. The limit curves in Option 2 of the BS-7910 and API-579 methodologies [1] [2] are provided in Equation (15), while the R6 procedure is defined in Equation (16) [3] [4].

$$(BS\ 7910)\ e\ (API\ 579)\ f(L_r) = \left(1 - 0,14(L_r^p)^2\right) \left\{0,3 + 0,7 \exp\left[-0,65(L_r^p)^6\right]\right\} \text{ to: } L_r^p \leq L_{r,max} \quad (15)$$

$$(R6) \begin{cases} f(L_r) = \left(1 + \frac{1}{2}L_r^2\right)^{-0,5} [0,3 + 0,7 \exp(-\mu L_r^6)] & \text{to: } L_r \leq 1 \\ f(L_r) = f(L_r = 1)L_r^{(N-1)/(2N)} & \text{to: } 1 < L_r \leq L_{r,max} \end{cases} \quad (16)$$

The safety assessment in the R6 methodology incorporates safe margins established in ASME Code Sec. III [5] and Sec. XI [16]. The new material limit curve is defined by equation (17), where the S_{FK} factor is established by ASME Code Sec. XI IWB-3612, with values of $\sqrt{10}$ for service classes A or B and $\sqrt{2}$ for service classes C or D [16].

$$F_{Lr,safe} = \frac{f(L_r)}{S_{FK}} \quad (17)$$

The safety factor against plastic collapse for local membrane and bending stresses SF_L^m is established by ASME Code Section XI in equation (18), derived from safety factor SF_L from ASME Code Sec. III. The term σ_f represents the average of the yield and rupture stress according to ASME Code Sec. XI [16].

$$SF_L^m = \frac{\sigma_f}{S_m C_p} \quad (18)$$

$$S_m = \min \left[\frac{2}{3} \sigma_y^{20^\circ C}, \frac{1}{3} \sigma_u^{20^\circ C}, \frac{2}{3} \sigma_y^{T^\circ C}, \frac{1}{3} \sigma_u^{T^\circ C} \right] \quad (19)$$

The term C_p is assigned by ASME Code Sec. III code [5] according to values assigned in Table 1.

Table 1 - Safety factors obtained from ASME Code Section III

SERVICE CLASS	C_p	f_1	f_2
A	1,0	1,5	1,5
B	1,1	1,8	1,5
C	1,5	2,25	1,8
D	2,0	3,0	2,0

Source: Adapted from ASME Code Sec. III [5].

The factor SF_L for ferritic steels is given in equation (20). The calculation of SF_L^b is provided by equation (21) [4] [3].

$$SF_L = SF_L^m \tag{20}$$

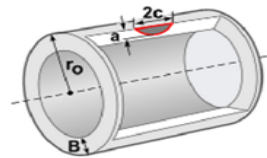
$$SF_L^b = \max \left\{ 1,0; \begin{cases} \frac{\frac{4}{f_1 \pi} * \sigma_f}{S_m} & \text{if, } f_1 S_m \leq f_2 \sigma_y \\ \frac{\frac{4}{f_2 \pi} * \sigma_f}{\sigma_y} & \text{if, } f_1 S_m \leq f_2 \sigma_y \end{cases} \right\} \tag{21}$$

The calculation of the L_r limit in safety assessment of the R6 procedure is given by $L_{r,max(safe)}$ according to equation (22).

$$L_{r,max(safe)} = \frac{L_{r,max}}{SF_L} \tag{22}$$

The study aims to evaluate semielliptical cracks on the external surface of the pressure vessel side, away from structural discontinuities as shown in Figure 2.

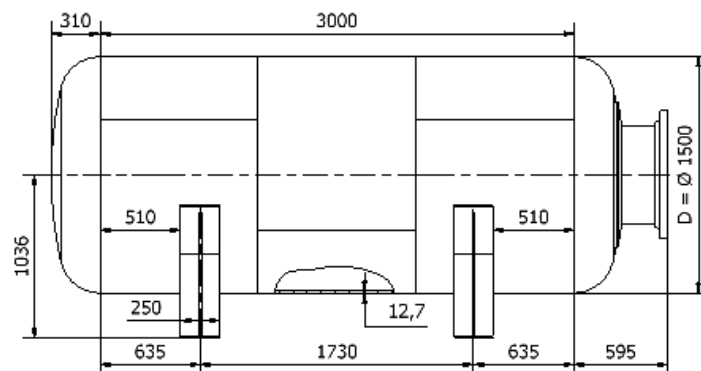
Figure 2 - External axial surface crack – semielliptical



Source: Printscreen from TWI Software Crackwise [23]

The case study of the SA-516 Gr 70 steel pressure vessel [20] is illustrated in Figure 3.

Figure 3 - Pressure vessel sketch



Source: Adapted from DSEED Engineering [18]

Table 2 shows data regarding material properties and geometry [10].

Table 2 - Pressure vessel data.

L [m]	D [mm]	t[mm]	P [MPa]	T _{proj} [°C]	E _{weld}	E [GPa]	σ _y [MPa]	σ _u [MPa]	ν
3	1500	12,7	1	200	0,7	195	340	567	0,3

Source: Authors

The algorithm converted into Matlab language statements was based on the sequence of steps described in Table 3 to determine FAD diagrams in option 2 of FFS methodologies.

Table 3 - Generic algorithm for developing the program in Matlab

INPUTS			
Pressure vessel dimensions	Stress analysis	Material data	Crack geometry
- Internal radius (R _i) - Thickness (t) - Length of the side (W)	- Primary membrane stress (P _m) - Primary bending stress (P _b) - Secondary membrane stress (Q _m) - Secondary bending stress (Q _b)	- Fracture toughness (K _{mat}) - σ _y at design temperature - σ _u at design temperature - Stress-strain curve - Plasticity data	- Crack depth (a) - Crack length (2c) - Ratio t/R _i - Ratio a/c - Ratio a/t
PROCESS			
- Determine failure assessment line - [f(L _r)] - Determine primary stress concentration factors at the crack tip and in the middle (K _i ^P) - Determine secondary stress concentration factors at the crack tip and in the middle (K _r ^S)	- Calculate reference stress (σ _{ref}) - Calculate loading ratio (L _r) - Calculate plasticity interaction factor (V) - Calculate fracture toughness ratio (K _r)		
OUTPUT			
-Plot points (L _r ,K _r) for cracks with depths (a) = 0.2; 0.4; 0.6 and 0.8 of the thickness (t)			

Source: Authors

Tables 4 and 5 summarize calculations relating to stress analysis in BS PD 5500 and ASME Code Sec VIII Div. 2 standards, respectively.

Table 2 - Stress analysis according to BS PD 5500

F _v [N]	M _v [N*mm]	σ _θ [MPa]	σ _z [MPa]	τ [MPa]	f ₁ [MPa]	f ₂ [MPa]	f ₁ +0,5p [MPa]	P _m [MPa]	Q _m [MPa]	Q _b [MPa]	P _b [MPa]
41378	3827511	58,1	30,3	0	58,1	30,3	58,6	58,6	262	13,9	2,0

Source: Authors

Table 3 - Stress analysis according to ASME Section VIII - Div. 2

F _v [N]	M _v [N*mm]	σ _{θm} [MPa]	σ _{sm} [MPa]	τ [MPa]	σ ₁ [MPa]	σ ₂ [MPa]	σ ₃ [MPa]	P _m [MPa]	Q _m [MPa]	Q _b [MPa]	P _b [MPa]
41378	3827511	83,7	42,4	0	83,7	42,4	-0,50	72,9	288,0	20,6	2,0

Source: Authors

Table 6 shows the nomenclature of terms used in figures, tables and equations.

Table 6 - Nomenclature

TERM	DESCRIPTION	TERM	DESCRIPTION
a	depth of crack-like flaw	Q _b	secondary bending stress
A ₀ to A ₃	coefficients stress distribution	Q _m	secondary membrane stress
A _p , p, P	internal vessel pressure	q _y	$[(\sigma_m M_m + \sigma_b M_b) / \sigma_y]^2 / 6$ (ASME XI)
C _p	permissible membrane factor	R _i , r _i	cylinder inside radius
D	pressure vessel diameter	R _m	cylinder mean radius
E	Young's modulus	R _o , r _o , R	cylinder outside radius
E _{weld}	welding efficiency	RT _{NDT}	maximum of the nil-ductility transition temperature
F	$1.12 + 0.053\alpha + 0.0055\alpha^2 + (1 + 0.02\alpha + 0.019\alpha^2)(20 - R_m/t)^2 / 1400$	SF _{L^b}	safety factor against plastic collapse for bending stresses
f(L _r)	failure assessment line	SF _{L^M}	safety factor for local membrane
f(L _{r,safe})	safety failure assessment line (R6)	SF _m	membrane safety factor (ASME XI)
f ₁	permissible global bending factor for S _m (ASME III)	S _m	allowable design stress
f ₁ , σ ₁	first principal stress	S _r	load ratio (ASME XI)
f ₂	permissible global bending factor for σ _y (ASME III)	T	temperature
f ₂ , σ ₂	second principal stress (BS-5500) and (ASME VIII)	t, B	wall thickness
f ₀ ^A , f ₁ ^A	stress concentration factors (R6)	T _{proj}	design temperature
F _p	peak stress	S _{FK}	safety factor against fracture
F _v	force acting in pressure vessel	SF _L	safety factor against plastic collapse
f _w	finite width correction factor	T _{ref}	reference temperature (FFS)
g	$1 - 20(a/2c)^{0.75} \alpha^3$ (API-579)	V	plastic correction factor (BS-7910)
G ₀ to G ₃	correction factors (ASME XI)	W, L	structural width in plane of flaw
G ₀ to G ₄	stress intensity factors (API-579)	α	(a/t)/(a/l) (API-579)
J _{IC}	critical J-value according ASTM-E1820	α''	a/W (BS-7910)
K _I	stress intensity factor	ζ	(a·l)/[t(l+2t)] (R6)
K _I ^P	primary stress intensity factor	μ	min(0.001E/σ _y , 0.6)
K _I ^S , K _I ^{SR}	secondary stress intensity factor	ν	Poisson's ratio
K _{mat} , K _{IC}	material fracture toughness	ρ	plastic correction factor (R6)
K _r , K _r '	toughness ratio	σ ₁ ^S	stress component in the first order polynomial
l, 2C	major axis of flaw	σ ₃	third principal stress
L _r	load ratio	σ _f	flow stress = (σ _y + σ _u)/2
L _{r,max}	cut-off to prevent plastic collapse	σ _h	pR _m /t
M	bulging correction factor	σ ₀ ^S	secondary bending stress
M _b	correction factor for bending stress	σ _{ref}	reference stress
M _m	correction factor for membrane stress	σ _u	ultimate tensile strength
M _s	stress magnification factors	σ _y , σ _{ys}	yield stress
M _v	moment acting in pressure vessel	σ _{ref} ^P	primary reference stress
N	$0.3(1 - \sigma_y / \sigma_u)$	σ _z , σ _{sm}	longitudinal stress
P _b , σ _b	primary bending stress	σ _{θm} , σ _θ	hoop stress
P _m , σ _o ^P , σ _m	primary membrane stress	τ	shear stress
Q	$1 + 4.593[a/2c]^{1.65} - q_y$ (ASME XI)	Φ	plastic correction factor (API-579)

The material toughness K_{mat} used in the BS-7910 methodology was considered to be 58.8 MPa (m)^{0.5} according to [13] and 84 MPa (m)^{0.5} for the API-579 and R6 methodologies. The K_{mat} value is estimated according to ASME Code Sec. XI (K_{IC}), which in the nuclear area is given by equation (23) [15] [16] and forms the basis for the calculation in the API-579 and R6 methodologies, as shown in equation (24). In these methodologies T_{ref} replaces RT_{NDT} for equipment not in the nuclear sector. The term RT_{NDT} is the reference temperature for zero ductility, obtained in Charpy test where rupture energy must be greater than 68 J and lateral expansion must exceed 0.89 mm [15] [16]. The term T_{ref} has the same meaning as RT_{NDT} , but the rupture energy of Charpy test must be greater than 28 J.

$$(ASME Sec. XI) \quad K_{IC} = 36,5 + 3,084exp[0,036(T - RT_{NDT})] \quad (23)$$

$$(R6) e (API 579) \quad K_{IC} = 36,5 + 3,084exp[0,036(T - T_{ref} + 56)] \quad (24)$$

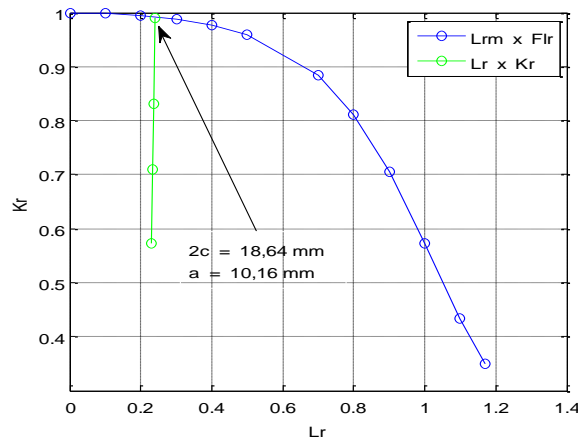
3. RESULTS AND DISCUSSIONS

The BS-7910 methodology provided the results illustrated in Figure 4 for FFS evaluation of an external axial (longitudinal) semielliptical crack. The green line on the graph represents a depth of 80% of thickness (10.16 mm), critical length of $2c = 18.64$ mm, close to the limit imposed by material properties as shown in the blue line. The parameter (c) corresponds to half the crack length, which can be changed in a computer program, so that the point corresponding to the maximum established depth ($a = 10.16$ mm) reaches the limiting line in the graph.

The API-579 methodology provided the result in Figure 5 for the FFS evaluation of an external axial (longitudinal) semi-elliptical crack. The light blue line on the graph represents the relationship $2c = 4a$. Therefore, for a depth of 80% of thickness (10.16 mm), the critical length is $2c = 40.64$ mm, close to the limit line. The red line represents the relationship $2c = 2a$, where for a depth of $a=10.16$ mm the critical length is $2c = 20.32$ mm,

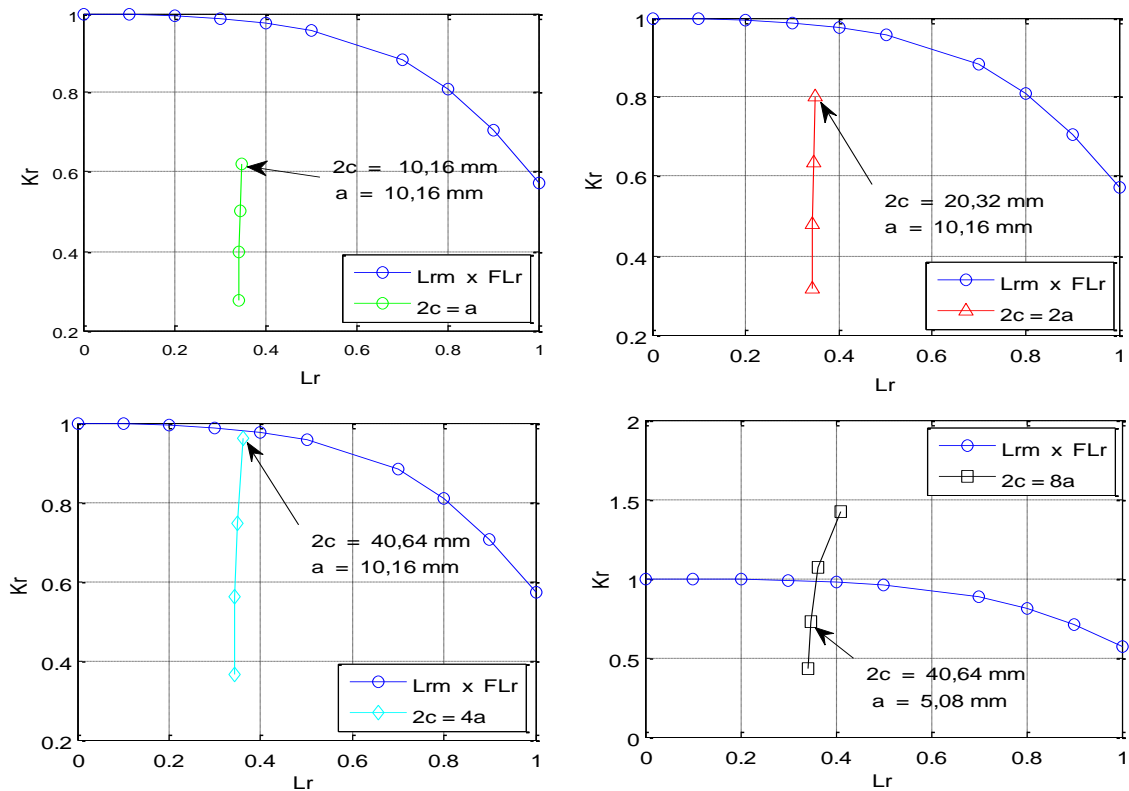
offering a more appropriate representation of the critical crack dimensions. In the BS-7910 methodology, the crack length is adjusted to reach the limit line, whereas in the API-579 methodology, predefined classes of critical crack depths and lengths are used.

Figure 4 - External axial (longitudinal) crack – Level 2 assessment of BS-7910 obtained in Matlab



Source : Authors

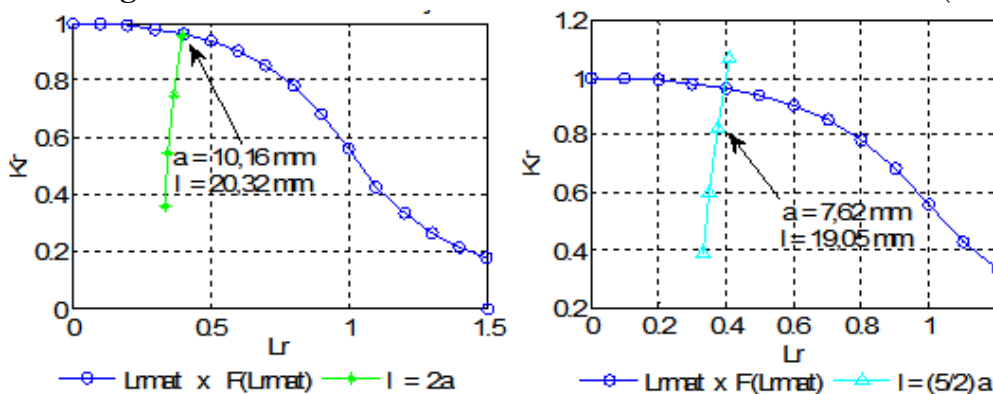
Figure 5 - External axial (longitudinal) crack – API-579 level 2 assessment obtained in Matlab



Source : Authors

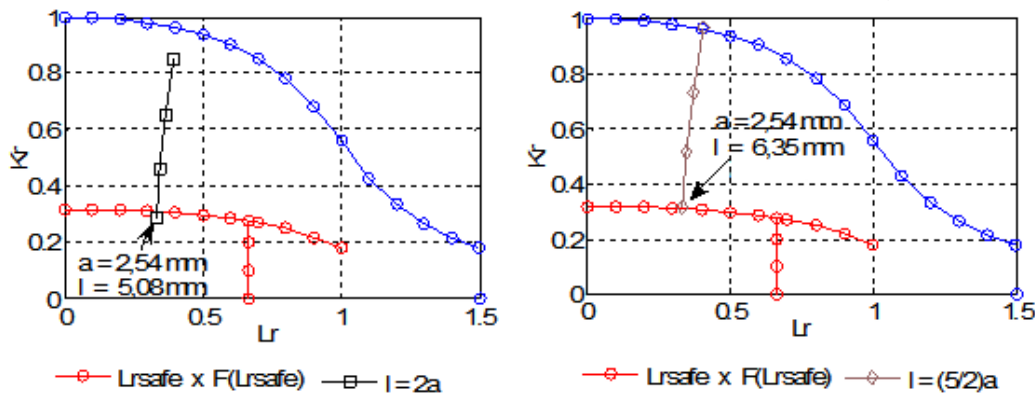
The R6 procedure presented results for the FFS evaluation of an external axial (longitudinal) semielliptical crack at level 2. A critical length of 20.32 mm was obtained for a normal evaluation at a critical depth of 10.16 mm, as shown by the green line in Figure 6. On the other hand, for service class A, the most safety-demanding category, at a critical depth of 2.54 mm (20% of the pressure vessel wall thickness), the critical length was 5.08 mm, as shown by the black line in Figure 7. Similarly to the API-579 methodology, the R6 procedure also uses predetermined classes of critical crack depths and lengths. The area below the dark blue boundary line is acceptable for a normal evaluation. However, for an evaluation considering safety margins for service class A equipment, only points located below the red line are acceptable.

Figure 6 - External axial crack – Level 2 - normal assessment of R6 (Matlab)



Source : Authors

Figure 7 - External axial crack – Level 2 - assessment for service class A equipment of R6 (Matlab)



Source : Authors

4. CONCLUSIONS

The assessment of the structural integrity of pressure vessels using FAD failure analysis diagrams, primarily with the aid of Matlab, has proven to enhance safety by determining the critical dimensions for detected or postulated cracks, as evaluated through FFS methodologies.

The computer programs developed in Matlab provide critical data for decision-making by analyzing and modifying geometric, material, and process characteristics to assess the damage tolerance of the evaluated equipment. The FFS methodologies studied are based on ASME Codes for pressure vessels and piping, particularly Sections III and XI.

Finally, an analysis of the three methodologies under the operating conditions of the case study concludes that, for normal evaluations, critical length ($2c$) up to 40.64 mm and depth (a) = 10.16 mm are acceptable for a pressure vessel diameter 1500 mm and total length of 3000 mm. However, for class A service equipment in the nuclear sector, only critical length (l) = 5 mm and depth (a) = 2.5 mm are permissible.

ACKNOWLEDGMENT

This work was made possible thanks to the support provided the Institute of Energy and Nuclear Research – IPEN-CNEN of São Paulo and the Navy Technological Center in São Paulo – CTMSP.

CONFLICT OF INTEREST

All authors declare that they have no conflicts of interest.

REFERENCES

- [1] BRITISH STANDARDS INSTITUTION- BSI - BS7910:2005 - **Guide to methods for assessing the acceptability of flaws in metallic structures**. London, 2005.
- [2] API 579-1/ASME FFS-1:2016 - **Fitness-For-Service**. “American Society of Mechanical Engineers”, New York, USA, 2016.
- [3] DILLSTRÖM, P., GUNNARS, J., VONUNGE, P., MÅNGÅRD, D., **Procedure for safety assessment of components with defects 2018:18** – Handbook Edition 5, Kiwa Inspecta Technology AB, Stockholm, Available at: www.stralsakerhetsmyndigheten.se.
- [4] R6:2015, **Assessment of the Integrity of Structures Containing Defects, R6 – Revision 4**, Up to amendment record No.11, EDF Energy Nuclear Generation Ltd.
- [5] ASME Code Section III, Division 1 - **Boiler and Pressure Vessel Code Rules for Construction of Nuclear Facility Components**, New York, NY, USA July, 2010.
- [6] MEDINA, J. A. H., **Evaluation of elastoplastic fracture predictions**, PhD thesis PUC, Rio de Janeiro-RJ, 2014.
- [7] MATTAR NETO M., CRUZ J.R.B., DE JONG R.P., **Influence of the materials mechanical properties on the structural integrity assessment of cracked piping of PWR nuclear reactors primary systems**, Progress in Nuclear Energy 50, 2008.
- [8] ASME Code Section VIII Division 1 - **Boiler and Pressure Vessel Code - Rules for Construction of Pressure Vessels**, New York, NY, USA July, 2010.
- [9] ASME Code Section VIII Division 2 - **Boiler and Pressure Vessel - Alternative Rules for Construction of Pressure Vessels**, New York, NY, USA July, 2010.
- [10] KUMAR, N.,ALSABBAGH, A., SEOK, C.S., MURTY, K.L., **Synergistic Effects of Neutron Irradiation and Interstitial Nitrogen on Strain Aging in Ferritic Steels**, The Minerals, Metals & Materials Society, 2017.
- [11] BSI PD 5500 - **Specification for Unfired Fusion Welded Pressure Vessels**, Fourth edition, UK, Jan 2009.
- [12] ANDERSON, T.L., **Fracture Mechanics – Fundamentals and Applications**, 4^a Edition, CRC Press, 2017.
- [13] SEOK, C., **Effect of temperature on the fracture toughness of SA-516 GR70 steel**, KSME international journal Vol. 14, N^o 1,pp. 11 a 18, 2000.

- [14] ZICK, L. P., **Stress Horizontal Cylindrical Pressure Vessels on Two Saddle Supports**, published in *The Welding Journal Research Supplement*, 1951.
- [15] MANESCHY, J. E., MIRANDA, C. A. J., **Fracture Mechanics in the Nuclear Industry**, Eletrobrás, Eletronuclear, Rio de Janeiro-RJ, 2014.
- [16] ASME Code Section XI - **Boiler and Pressure Vessel - Rules for in Service Inspection of Nuclear Power Plant Components**, New York, NY - USA, 2010.
- [17] TINOCO, E., PATRÍCIO, N., FREIRE, P. S., **Design and Stress Analysis Codes for Pressure Vessels**, PETROBRAS.
- [18] DSEED ENGINEERING, **Data-Book Handbook**, Sorocaba-SP, 2011.
- [19] MIRANDA, C. A. J., Thesis presented to IPEN, **Obtaining the Cleavage Stress and Reliability Level in Determining the Reference Temperature Transition of Ferritic Steels: Numerical and Experimental Approach**, São Paulo, 1989.
- [20] AMERICAN SOCIETY FOR TESTING MATERIALS - ASTM A516 Carbon Steel, Grade 70.
- [21] MATTAR NETO M. **An approach to defining criteria, codes and standards for the mechanical and structural design of nuclear power plant components**, IPEN-CNEN, São Paulo-SP.
- [22] JASKE, CARL E., KOCH, G. H., **Failure and Damage Mechanisms - Embrittlement, Corrosion, Fatigue and Creep**, Cortest Columbus Technologies, Inc, Columbus, Ohio.
- [23] TWI Software. Crackwise 5 help content version 5.0 27934 Final, 2016.
- [24] ASME Code Section II - **Boiler and Pressure Vessel – Part D – Properties - Materials**, New York, NY, USA July, 2010.

LICENSE

This article is licensed under a Creative Commons Attribution 4.0 International License, which permits use, sharing, adaptation, distribution and reproduction in any medium or format, as long as you give appropriate credit to the original author(s) and the source, provide a link to the Creative Commons license, and indicate if changes were made. The images or other third-party material in this article are included in the article's Creative Commons license, unless indicated otherwise in a credit line to the material. To view a copy of this license, visit <http://creativecommons.org/licenses/by/4.0/>.